Lasers in Manufacturing Conference 2015

Effect of processing parameters in welding of biocompatible polymer film to metal sheet using an infrared laser source

Hui-Chi Chen*, Guijun Bi, Juan Carlos Hernández Castañeda, Hong Xie, Jun Wei

Singapore Institute of Manufacturing Technology, 71 Nanyang Drive, Singapore 638075.

Abstract

Miniaturisation and light weight design has become one of the key trends in today's manufacture industry. This transformation is also happening in the medical instrumentation industry. In addition to size and weight reduction, biocompatibility and hermetic sealing are other common quality requirements for medical applications. Laser welding is a unique non-contact joining process which yields a high precision weld with small heat-affected zone. This work employs an infrared laser source for generating micro-scale welds. Process development of micro laser welding of dissimilar biocompatible materials is reported herein. The optimisation of parameters and different weld designs are investigated. The micro laser welding process developed targets the joining of heat-sensitive miniature devices that require air-tight joining quality.

Keywords: Laser welding; biocompatible; dissimilar materials.

1. Introduction

The recent trend in medical industry is gradually moving towards miniaturisation and function/design flexibility. Manufacturers are therefore developing micro-scale processes needed in the production of miniaturised medical devices. In addition to size reduction, the devices are frequently designed and fabricated with hybrid materials. This given their functional requirements, such as anti-stress corrosion cracking, signal transmission and wireless power charge, needed for medical devices (Bombač et al., 2007). In comparison to conventional joining methods (i.e. mechanical fastens, adhesive or ultrasonic bonding),

* Corresponding author. Tel.: +65 6793 8345; fax: +65 6793 8383.
E-mail address: hcchen@SIMTech.a-star.edu.sg.

laser welding, a non-contact joining process, provides advantages on producing a joint with high precision, strength and flexibility. Furthermore, the joints show biocompatibility and long-term stability.

In laser lap welding of transparent polymer to metal materials, a laser beam passes through the polymer and irradiates the top surface of the metal. Light energy absorbed by the metal is transformed into heat energy and conducted to the surrounding areas including the polymer side. With sufficient heat input, the polymer melts and moist onto the metal surface. A joint is therefore performed. The main obstacle in laser welding of polymer to metal materials is given by their different optical and physical properties. A narrow processing window is expected for this joining process as in one hand, the polymer material can be easily damaged and decomposed if excessive heat is applied. On the other hand, an unreliable joint is created when insufficient heat input is applied in the process. Although laser welding of polymer to metal materials has been the subject of continuous developments in recent years, most research works focussed on generating macro-scale joints using near infrared laser sources. Limited research has been conducted in micro laser welding of polymer to metal.

An 807 nm wavelength diode laser source was shaped into a line beam for laser lap welding of 2.0 mm thick PET laminate and 3.0 mm thick 304 stainless steel plate by Katayama and Kawahito, 2008. They developed a joint with 3 kN shear strength. However, the average dimension of their welds were about 6 mm by 30 mm. Farazila et al. ,2011 demonstrated laser spot welding of 0.5 mm thick PET sheet to 2.0 mm thick SUS 304 stainless steel plate by a pulse wave Nd:YAG laser. They indicated that joint strength was related to the amount of heat input absorbed by stainless steel and the size of heat affected zone. Hussein et al., 2013 investigated the weld quality of 2 mm thick PMMA to 1 mm thick 304 stainless steel laminate in pulsed Nd:YAG laser welding. Their results show that the joint strength improved by increasing heat input. However, over increasing the heat input caused polymer degradation, bubble formation as well as reduced joint strength. Surface treatments, such as anodising, have been explored to improve joint strength. Farazila et al., 2012 improved the joint strength in laser lap welding of 0.5 mm thick PET to 1 mm A5052 aluminium alloy laminate by anodising the surface of the latter. In addition, they mentioned that adequate bubbles formed near the joining interface may have contributed to the improvement of the joint strength. Here, the inner pressure generated by bubbles pressed and spread the molten polymer onto the metal. Miyashita et al., 2009 performed laser welding of different polymer materials to stainless steel plate. They also indicated that bubbles played a role to press polymer material to the metal during the molten and softened stages. Katayama and Kawahito, 2010 further studied the bonding mechanisms in laser welding of polymer to metals. They found that the oxide film on the metal surface played an important role at atomic and molecular level joining. Not only the mechanical interlocking effect, but the Van der Waals interaction force and chemical bonding contributed to the overall bonding mechanisms.

The aim of this work is to investigate the relationship between process parameters and weld quality in pulse wave (PW) Nd:YAG laser micro welding of PET film to stainless steel sheet. Experimental results show that a micro weld with good weld appearance and quality was achievable by using an infrared PW Nd:YAG laser source. The strength and sealing capability of the joints was closely related to percentage area covered by the generated bubbles in the welds. The formation of these bubbles was dominated by the amount of heat input (a function of average pulse energy, pulse frequency, pulse duration and welding speed) applied in the laser welding process.

2. Materials and Methods

Laser lap welding of 0.125 mm thick PET film to 0.6 mm thick 304 stainless steel sheet was conducted by using an infrared pulse wave Nd:YAG laser. Physical properties of both welding materials are summarised in Table 1. Before laser welding, PET and stainless steel were cleaned with Isopropyl alcohol solvent. The

welding conditions used in this work are tabulated in Table 2. Throughout this work, the focal point position of the laser beam was positioned on the top surface of stainless steel. The pulse frequency was varied from 60 Hz to 80 Hz while the rest of the process parameters were kept constant. Each welding condition was repeated three times to ensure their process stability.

Table 1 Physical properties of PET and 304 stainless steel

Material properties	PET	304 stainless steel
Melting point (°C)	243-260	1399-1454
Density (kg/cm^3)	1455	8000
Specific heat (J/kg K)	1000	880
Thermal conductivity (W/m K)	0.24	138
Coefficient of thermal expansion (10^{-5} /°C)	6.0	1.72
Surface roughness (μm)	0.0031	0.0919

Table 2 Summary of laser welding conditions used in this work.

Welding condition No.	1	2	3
Pulse energy (J)	0.63	0.63	0.63
Pulse Frequency (Hz)	60	70	80
Pulse duration (ms)	1.5	1.5	1.5
Average power (W)	37.5	44.0	50.0
Speed (mm/min)	1500	1500	1500

After laser welding, weld appearance and dimension were investigated by Olympus SZ optical microscopy. Surface roughness and the welds' profiles were measured by a Talysurf 200 precision measurement system. After the aforementioned non-destructive inspections, welds were cross-sectioned, mounted and polished for further examinations. Weld strength was evaluated by means of pull tests with an INSTRON 5548 universal testing machine. The fractured surface from the PET side of the welds was observed by optical microscope equipped with analySIS® software. Sealing tests of the welds were conducted according to the *ASTM F 1929* standard*: Standard test method for detecting seal leaks in porous medical packaging dye penetration*. Finally, the chemical composition of the welds was analysed by Raman spectroscopy.

3. Results and Discussion

3.1. Weld appearance and geometry

A macro image of a laser lap welded PET film to stainless steel sheet is presented in Figure 1(a). No obvious melt flash or burn marking was observed on the top surface of PET. Figure 1(b) shows the top view of a weld obtained at the pulse frequency of 70 Hz. Bubbles with various sizes were formed within laser spots. The relationship between pulse frequency and weld width is summarised in Table 3. By increasing the pulse frequency from 60 Hz to 80 Hz, the weld width increased from 537 µm to 607 µm.

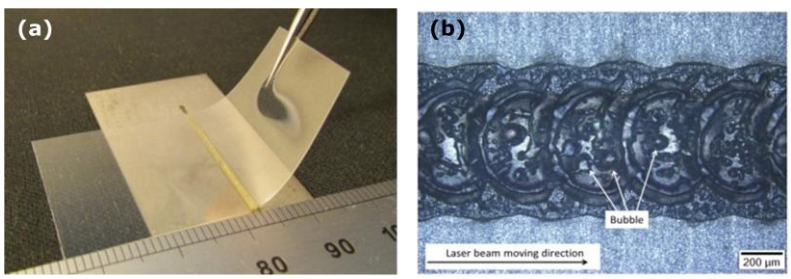

Figure 1 Laser lap welded of PET film to stainless steel (a) and a micro image from top view of the weld (b).

Table 3 Evaluations of the welds

Pulse frequency (Hz)	Weld width (µm)	Surface roughness of the welded PET film (µm)	Break load at break (N)	Area percentage covered by bubbles on the fractured PET side (%)
60	537	0.0035	27.58	12.42
70	591	0.0038	93.39	51.61
80	607	0.8220	71.95	66.30

Figure 2(a) is a magnified image of a weld from Figure 1(b). Bubbles of various sizes are clearly observed. Here, the biggest bubble is surrounded by multiple smaller bubbles. After laser welding, the PET (presented in RED colour) remaining in the weld is shown in Figure 2(b). PET is evenly distributed in the weld except in the area where bubbles formed.

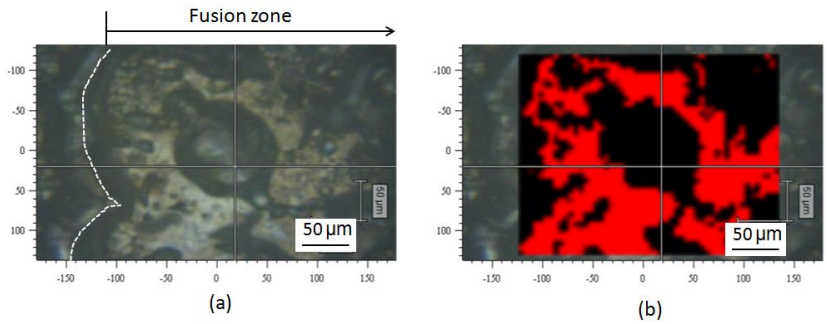

Figure 2 A magnified image of a weld from the top view (a); residual PET (RED colour) material distributed near bubbles (b).

Cross-sectional welds obtained at different pulse frequency are compared in Figure 3. By increasing the pulse frequency from 60 Hz to 80 Hz, the height of the molten area in the PET side increased from 47 µm (Figure 3(b)) to 100 µm (Figure 3(d)). In comparison to the surface condition of as-received stainless steel in Figure 3 (a); its top surface, near the joints' interlayer, became rougher when a higher pulse frequency was applied in the laser welding process as shown in Figure 3(b)-(d).

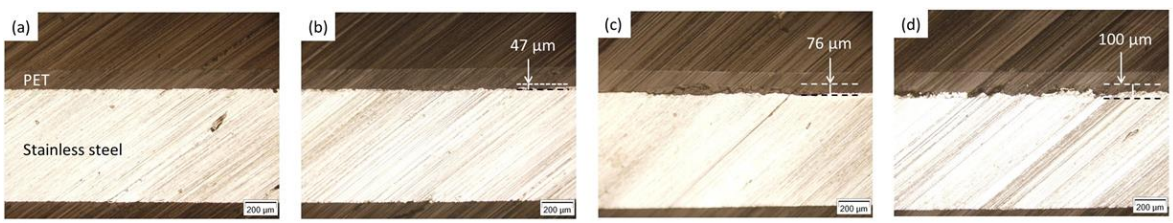

Figure 3 Cross section of welds obtained at different pulse frequency: (a) before laser welding; (b) 60 Hz; (c) 70 Hz; (d) 80 Hz.

Surface roughness on the top surface of laser welded PET films are provided in Table 3. For as-received stainless steel sheet and PET film, their average surface roughness were 0.0919 µm and 0.0031 µm, respectively. Surface roughness did not have significant change when pulse frequency of 60 Hz and 70 Hz were applied in laser welding. However, at 80 Hz, the roughest weld surface was obtained (0.8220 µm).

In order to investigate the deformability of the PET films in the laser welding process, the profiles of the welds under different conditions were measured and plotted in Figure 4. When 60 Hz was applied, the welded PET film was formed in a convex shape, as shown in Figure 4 (a). The peak point, 0.1328 µm above the reference plan, was observed at the centre of the weld. Figure 4 (b) shows a concave shape obtained at 70 Hz. The lowest point, 5.4128 µm below the reference plan, was observed near centre of the weld. Figure 4 (c) shows a similar concave shape obtained with pulse frequency of 80 Hz. The lowest point also was also observed near the centre of the weld with the value of 48.3678 µm below the reference plan.

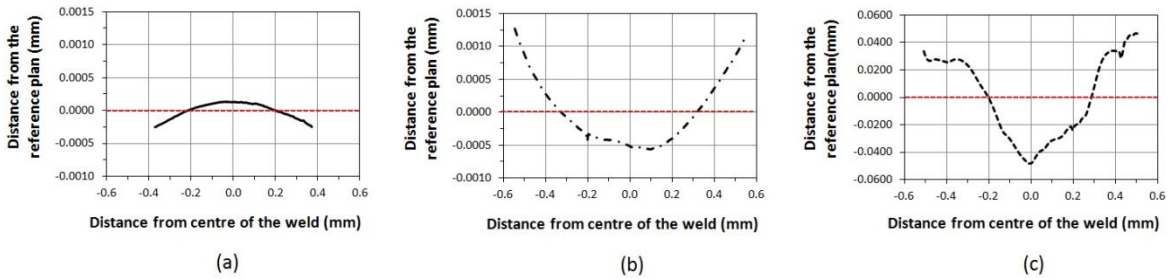

Figure 4 Weld profiles obtained under different pulse frequency: (a) 60 Hz; (b) 70 Hz; (c) 80 Hz.

3.2. Weld leakage and strength

Results of dye penetration tests are shown in Figure 5. When the pulse frequencies were kept at 60 Hz and 70 Hz, no black ink passed through the welds as shown in Figure 5(a) and Figure 5(b), respectively. When the pulse frequency increased to 80 Hz, on the contrary, black ink penetrated into the weld at various locations as indicated in Figure 5(c) and Figure 5(d). The leaks actually happened at locations where laser spots were overlapped.

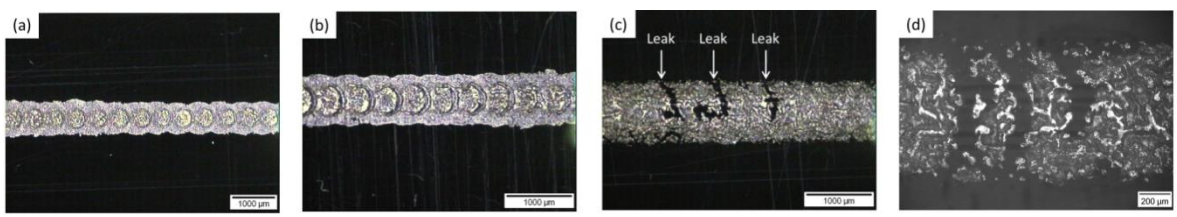

Figure 5 Dye penetration test of welds with different pulse frequency: (a) 60 Hz; (b) 70 Hz; (c) 80 Hz; (d) a high magnification image of Figure 5 (c).

Results of average break load of welds are summarised in Table 3. The highest break load (93.39 N) was obtained when 70 Hz was applied in laser welding. The weakest weld, 27.58 N, was found under the welding condition of 60 Hz. After pull tests, the fractured welds obtained from different pulse frequencies are presented in Figure 6 and Figure 7. Figure 6(a) shows the fractured surface from the PET side under pulse frequency of 70 Hz. Clear fusion and heat-affected zones are observed. A high magnification image of the joint and its heat-affected zone is presented in Figure 6 (b). The average bubble size at the heat-affected zone was smaller than those in the fusion zone. Figure 6 (c) shows a high magnification image of the fusion zone. Its area percentage of bubble was around 61% as listed in Table 3.

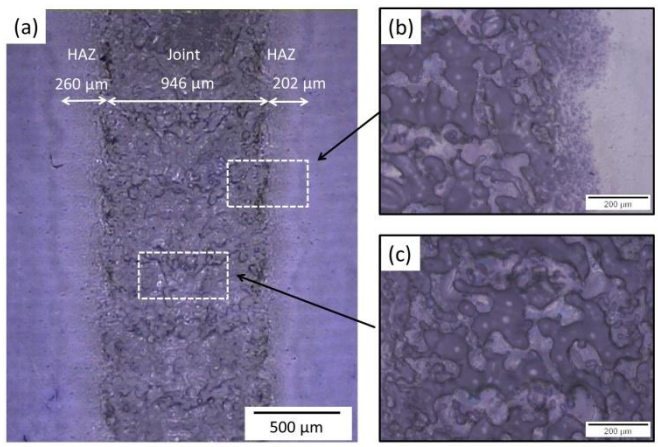

Figure 6 A fractured surface from the laser welded PET film (a); a higher magnification image of the fusion and heat-affected zone (b); a higher magnification of the fusion zone (c). (Pulse frequency: 70 Hz).

Figure 7 shows the fractured surface from the PET side under pulse frequency of 60 Hz. In comparison to Figure 6(a), both fusion and heat-affected zones of the welds are narrower in Figure 7(a). In addition, the boundary between each laser spot is clearer as shown in Figure 7(b). Under this welding condition, bubbles were mainly formed at the laser spot overlapping areas. The area percentage of bubble was around 12% which was lower than those formed under pulse frequency of 70 Hz and 80 Hz as listed in Table 3. By increasing the pulse frequency, the area percentage of bubble in the joints increased.

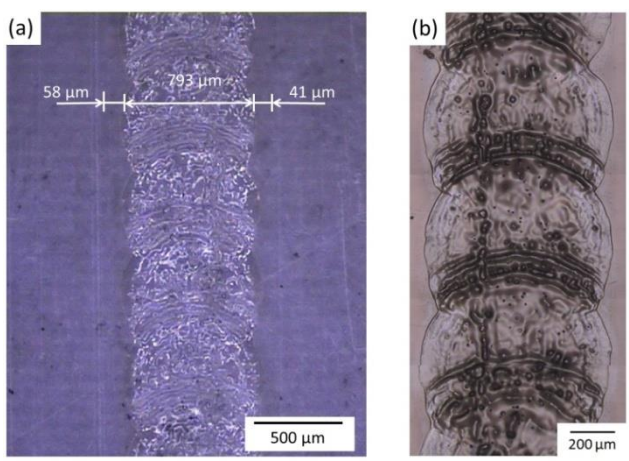

Figure 7 A fractured surface from the laser welded PET film (a); a higher magnification image of the fusion and heat-affected zone (b). (Pulse frequency: 60 Hz).

4. Discussion

In laser lap welding of PET film to stainless steel sheet, the main challenge is to precisely deliver laser energy at the interlayer between the two welding materials. The heat input should be sufficient to melt the PET film, but not causing any degradation on it. In general, heat input is a function of the average power, pulse energy, pulse duration, pulse frequency as well as the welding speed. In this study, the relationship between average power and weld quality was investigated by changing the pulse frequency. Figure 8 illustrates the welding seam generated in PW laser welding process with different pulse frequency.

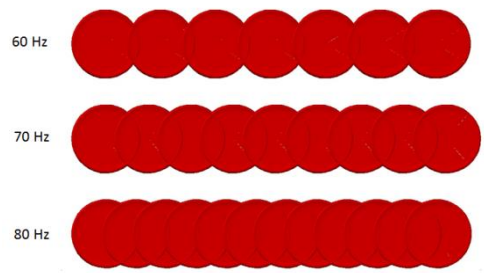

Figure 8 Schematic of welding seam generated in laser welding with different pulse frequency

When welding speed was kept constant, the pulse overlapping rate and average laser power increased with an increase of the pulse frequency, as illustrated in Figure 8. Since the heat accumulated at the laser spot overlapping area was higher than other locations, more bubbles were formed at those overlapping areas (Figure 7(a)) resulting in the generation of gas pressure. The gas pressure can press the PET film away from the interlayer (Figure 4(a)) if small amount of bubbles were formed. On the contrary, when sufficient bubbles were formed, the gas pressure contributed to press molten polymer to stainless steel and resulted in an increasing fusion zone and enhancement of the joint strength (Table 3). Instead of pressing the PET film away from the interlayer, the PET film was joined firmly on the stainless steel surface, as shown in Figure 4 (b)-(c). When the laser spot overlapping rate was increased, the amount of bubbles in the welds increased and they were evenly distributed on them (Figure 6(a)). If the laser spot overlapping rate reached a certain value, bubbles formed in the welds easily combined together as a new colony. The colony can be considered as an open channel across a weld where leakage was observed during dye penetration tests (Figure 5(d)).

From the experimental results, the average power not only affected weld size and bubble formation, but also surface roughness of stainless steel near the interlayer. The surface roughness of stainless steel was modified after laser welding, as shown in Figure 3. In principle, a rougher surface can enhance the mechanical interlocking effect between the PET film and the stainless steel sheet. At the same time, the formation of bubbles in the weld was also determined by the average power applied in the welding process. With an increment of the average power, the area percentage covered by bubbles increased (Table 3). The bubbles formed in the welds can cause pressure over the molten polymer to the stainless steel which increases the joint strength. However, when the area percentage of the bubbles in a weld passes a certain level, the joint strength will decrease given the lack of polymer remaining on the stainless steel.

Further investigation on the role of bubble formation and their effect on the weld quality will be conducted. The thermal effects on the PET film will be also analysed. Finally, different alternatives to restrict the formation of bubbles in the welds will be identified.

5. Conclusions

Pulse wave Nd:YAG laser welding of biocompatible PET film to stainless steel sheet has been successfully performed without any melt flash over the surface of PET film. The effect of pulse frequency and average power in determining the quality of the welds were investigated. Primary conclusions are summarised below,

- Average laser power which is a function of pulse frequency played an important role in determining the quality of the welds in terms of surface roughness, weld profile, bubble formation, weld strength as well as sealing capability.
- The weld profile can reflect the percentage area covered by bubbles resulting in the generation of gas pressure at the interlayer of joints.
- Weld strength and sealing capability were affected by the percentage area covered by bubbles in the welds.

Acknowledgements

The project was supported by Precision Engineering Centre of Innovation (PE COI), Agency for Science, Technology and Research (A*STAR), Singapore. Authors would like to thank Ms Liu Yuchan, Mr Pan Dayou and Mr Cheng Chek Kweng for their technical support during this work.

References

Bombač, D., Brojan, M., Fajfar, P., Kosel, F., Turk, R., 2007. Review of materials in medical applications, RMZ – Materials and Geoenvironment 54, p. 471-499.

Farazila, Y., Miyashita, Y., Hua, W., Mutoh, Y., Otsuka, Y., 2011. Journal o Laser Micro/Nanoengineering 6, p.69-74.

Farazila, Y., Miyashita, Y., Hua, W., Mutoh, Y., Mohd Hamdi, A., Effect of anodising on pulsed nd:YAG laser joining of polyethylene terephthalate (PET) and aluminium alloy (A5052), Journal of Materials & Design 37, p. 410-415.

Hussein, F., Akman, E., Genc Oztoprak, B.,Gunes, M., gundogdu, O., Kacar, E., Hajim, K., Demir, A., 2013. Evaluation of PMMA joining to stainless steel 304 using pulsed nd:YAG laser, Journal of Optics & Laser Technology 49, p. 143-152.

Katayama, S., Kawahito, Y., 2008. Laser direct joining of metal and plastic, Journal of Scripta Matrialia 59, p. 1247-1250.

Katayama, S., Kawahito, Y., 2008. Characteristics of LAMP joining structures for several materials, The 29th International Congress on Applications of Lasers & Electro-Optics (ICALEO 2010) Congress Proceedings. California, USA, Paper P169.

Miyashita, Y., Takahashi, M., Takemi, M., Oyama, K., Mutoh, Y., tanaka, H., 2009. Journal of solid mechanics and materials engineering 3, p. 409-415.